

Finite element analysis of drilling unidirectional CFRP in different ply orientation

H. Sanusi^{1*}, M.S. Hussin¹, A.R. Yuzairi¹, A. Azmi¹, L. H. Peng¹ and M.F.A. Ahmad²

¹ Faculty of Mechanical Engineering Technology, Universiti Malaysia Perlis, Kampus Tetap Pauh Putra, 02600 Arau, Perlis, Malaysia

² School of Engineering, Faculty of Science and Technology, Quest International University, 30250 Ipoh, Perak, Malaysia

ABSTRACT – In the new era of Industrial Revolution 4.0 (IR 4.0), the manufacturing processes are facing a new level of flexible mass production technologies. Hence, the high demands for simulations data of manufacturing production and operation are required for developing a Cyber-Physical Systems of smart machines. Some composite machining processes could be very expensive. Simulation is needed to reduce the manufacturing time and cost. Without considering the suitable parameter of drilling, damage occurs at the region over the hole's boundary after the drilling operation is done. Thus, the goal of this research is to investigate the effects of drilling cutting parameter such as thrust force, drilling-induced damage and stress distribution of reinforcing carbon composite polymer (CFRP) laminate by developing a user-defined material model (VUMAT) subroutine in ABAQUS/EXPLICIT (ABAQUS, Dassault Systèmes®) for different fibre ply orientations. The failure mode such as fibre tensile failure, fibre compressive failure, matrix cracking and matrix crushing was modelled and analysed based on Hashin and Puck's criterion. The stages of drilling operation were observed and described in this paper with the drilling cutting parameter and the damage of composite was finely defined. The results proved that the relationship of thrust force is directly proportional to the feed rate with the difference of computational model are 8 % higher than the experiment. Among the ply orientation sequence applied in the simulation, the result shows that $[0_4/45_8/0_4]$ and $[45_4/-45_8/45_4]$ ply having higher thrust force with 401.84 N.mm and 390.53 N.mm at 500 mm/min feed rate as delamination extent, as the frequency of fiber pulls out at the exit region of the drilled hole increases as compared to the restricted fiber ply orientation 0° and 90° .

ARTICLE HISTORY

Revised: 17th Jul 2020

Accepted: 15th Aug 2020

KEYWORDS

Finite Element;
composite drilling;
ply orientation;
thrust force;
VUMAT subroutine

INTRODUCTION

Drilling is a prevalent secondary manufacturing or machinery process to create a through the hole at the surface of a workpiece. Nowadays, there are complete data sheets of drilling parameter for most metal which can be easily access from an online source, yet the data of drilling on the composite still need to be explored. This is due to the anisotropy and heterogeneity properties of the composite [1]. Appropriate cutting parameters during drilling can reduce the tool wear and minimize the damage occurring around the hole [2,3]. Even though the issue of drilling caused damage is normal to entire groups of composites, the most impacting parameters of the damage mode were rely upon the sort of composite [4]. The capability of the composite to be machining was primarily to be influenced by the orientation and properties of fibres and matrix [5].

In general, composite materials are usually described as a combination of two or more element, which their physical or chemical composition varies in their properties [6]. The orientation of ply can be categories into two, which are unidirectional and cross plied quasi-isotropic. Unidirectional CFRP was the workpiece chosen in this research. In the group of the problem that caused in composite structure by the drilling process, delamination is the most undesirable critical failure. Delamination happened mostly is because the drill point attack was located in the localized bending zone. Besides, as the consequences of the physical properties of the material, the damage is hard to observe and identified by visual inspection. This results in the requirement of non-destructive testing (NDT) to obtain the soundness of the parts. The damage created at the inlet of the drilled hole is represented by the delamination factor, which is investigated by examining feed rate, cutting speed and point angle as affecting process parameters [7,8]. Delamination can be curtailed by applying suitable cutting parameters.

It had proved that to prevent the risk of delamination occurs in the drilling process, the thrust force exerted by the drill chisel edge has to be reduced. No doubt that to minimize damage extension in a composite structure, the feed rate has to be kept as low as possible. The purpose of this condition needs to be considered to minimize the undesired thermal damages that cause from the matrix softening and to fulfil the technical terms, which are to ensure a practical number of hourly productions [2,9]. From this point of view, the appropriate thrust force exerts on the workpiece in drilling is important to optimize and maintain the quality of composite. The delamination mechanisms can be categorised into two types, which were peel- up and push-down, either occurred at the drill exit or entrance laminate side. Peel-up of a composite is due to the cutting force pushing the scrape and cut materials to the flute surface. At the beginning of the drilling process, the drill bit's cutting edge will wear away the laminate [3]. When the drill moves forward, it will pull the

scrape along with the flute, and before the material being effectively cut out it will spiral up. This action leads to detaching the upper laminas of the plate and thus creates a peeling force upwards [9].

The push-down occurs in the composite is due to the compressive thrust force of the drill's chisel edge consistently acts on the workpiece. During the drilling process, the laminate under the drill can isolate from the upper plies, thus breaking off the interlaminar bond will occur at the region around the hole. As the drill move closer to the end of the laminate, the thickness of the uncut part reduced, and weakens the capability to resist deformation. At a certain area before the drill is completely penetrated the laminate, as the force acted was greater than the interlaminar bond strength, it tends to happen delamination [9,10].

In general, Composite materials are usually described as a combination of two or more element, which their physical or chemical composition varies in their own properties [6]. The orientation of ply can be categories into two which are unidirectional and cross plied quasi-isotropic as shown in Figure 3. Unidirectional Carbon Fibre Reinforce Polymer was the workpiece chosen in this research. Due to the ultimate strength of CFRP in terms of excellent fatigue resistance and stiffness, CFRP composites are incredibly supportive of manufacturing the component that required lightweight and can improve the efficiency of structural in the fields of transportation, aerospace, sports equipment, etc. [11].

Applied Finite element analysis method in numerical models of drilling was developed to determine inter-laminar in composites [12]. A report on machining models of various styles of composites was published by Purdue University. In numerical modelling, once the model is authenticated to be functional it could be a useful tool to determine the parameters that influencing the drilling system and providing ominous prediction to evaluate the variables [13].

Numerical simulation is able to minimize the practical experimental budget and no doubt that efficiency will be enhanced [14]. Thus, the finite element method (FEM) is important in analyzing the damage of composite in terms of micro-scale. The study of material removal in orthogonal cutting and fracture of CFRP by using FEM was carried out by Van Luttervelt et al. [15] and Mahdi et al. [16]. A review of on FEM for machining such as turning, milling, drilling and orthogonal cutting was sorted out [17]. In this study, the focus was to evaluate different ply orientations to evaluate the delamination effect upon drilling.

METHODOLOGY

The finite element analysis was used to visualize the delamination prediction behaviour. The following steps in Figure 1 simulate the composite drilling. The drilling model consisted of three components which were flutes drill bit, and UD-T300/LTM45-EL laminate ply and a backing plate as in Figure 2. The simulation set up is explained in great detail in the next paragraph and replicated exactly as in Phadnis et al. [18].

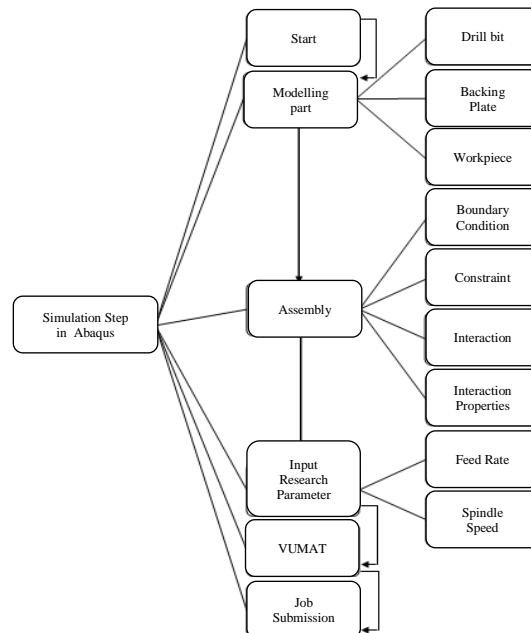


Figure 1. Flow chart of FEA in ABAQUS (ABAQUS, Dassault Systèmes®)

Material Modelling

A model of composite developed was an orthotropic homogeneous material of Unidirectional (UD) epoxy/carbon fibre laminate T300/LTM45-EL with 60% fibre content. The material and mechanical properties of T300/LTM45-EL were obtained from the literature demonstrated by Phadnis et al. [18]. A user-defined 3D damage model (VUMAT) subroutine with solid elements was developed based on the material characteristic of T300/LTM45-EL and applied to the

FE code ABAQUS/EXPLICIT (ABAQUS, Dassault Systèmes®) to predict the character and extent of damage through the laminate thickness.

Damage Initiation Criterion

To investigate the failure of composite, the Hashin failure criteria were applied for a unidirectional (UD) composite. In this research, Hashin failure criterion was applied to determine the failure in fibre. The previous study shows that the Hashin's criterion was used to estimate fibre damage, and another criterion named Puck's failure criterion was used to model matrix failure. These two criteria were applied in a user-defined material model (VUMAT) in the general-purpose finite element software ABAQUS/EXPLICIT (ABAQUS, Dassault Systèmes®). There are six different types of failure modes which are compressive fibre failure, compressive matrix failure, interlaminar compression failure, tensile fibre failure, tensile matrix failure, and interlaminar tensile failure as represented in Eq. (1), (2), (3), (4), (5) and (6) respectively [19,20].

i. Tensile fibre failure for $\sigma_{11} \geq 0$

$$\left(\frac{\sigma_{11}}{X_T}\right)^2 + \frac{\sigma_{12}^2 + \sigma_{13}^2}{S_{12}^2} = \begin{cases} \geq 1 & \text{failure} \\ < 1 & \text{no failure} \end{cases} \quad (1)$$

ii. Compressive fibre failure for $\sigma_{11} < 0$

$$\left(\frac{\sigma_{11}}{X_C}\right)^2 = \begin{cases} \geq 1 & \text{failure} \\ < 1 & \text{no failure} \end{cases} \quad (2)$$

iii. Tensile matrix failure for $\sigma_{22} + \sigma_{33} > 0$

$$\frac{(\sigma_{22} + \sigma_{33})^2}{Y_T^2} + \frac{\sigma_{23}^2 - \sigma_{22}\sigma_{33}}{S_{23}^2} + \frac{\sigma_{12}^2 + \sigma_{13}^2}{S_{12}^2} = \begin{cases} \geq 1 & \text{failure} \\ < 1 & \text{no failure} \end{cases} \quad (3)$$

iv. Compressive matrix failure for $\sigma_{22} + \sigma_{33} < 0$

$$\left[\left(\frac{Y_C}{2S_{23}}\right)^2 - 1\right] \left(\frac{\sigma_{22} + \sigma_{33}}{Y_C}\right) + \frac{(\sigma_{22} + \sigma_{33})^2}{4S_{23}^2} + \frac{\sigma_{23}^2 - \sigma_{22}\sigma_{33}}{S_{23}^2} + \frac{\sigma_{12}^2 + \sigma_{13}^2}{S_{12}^2} = \begin{cases} \geq 1 & \text{failure} \\ < 1 & \text{no failure} \end{cases} \quad (4)$$

v. Interlaminar tensile failure for $\sigma_{33} > 0$

$$\left(\frac{\sigma_{33}}{Z_T}\right)^2 = \begin{cases} \geq 1 & \text{failure} \\ < 1 & \text{no failure} \end{cases} \quad (5)$$

vi. Interlaminar compression failure for $\sigma_{33} < 0$

$$\left(\frac{\sigma_{33}}{Z_C}\right)^2 = \begin{cases} \geq 1 & \text{failure} \\ < 1 & \text{no failure} \end{cases} \quad (6)$$

Where σ denoted the stress component with respect to material principal axes, X_T, X_C, Y_T and Y_C are the longitudinal tensile strength, longitudinal compressive strength, transverse tensile strength and transverse compressive strength respectively. Furthermore, S_{12} and S_{23} represent the longitudinal shear strength and transverse shear strength respectively. The failure criterion of Puck was applied to model and investigate matrix failure. Based on the theory founded by Schurmann and Puck the damage model capable of predictive the failure criteria in unidirectional laminates [21]. The mathematical equation of Puck's criteria for failure in brittle epoxy matrix failure was as shown below.

$$\left[\left(\frac{\sigma_{11}}{2X_{1t}}\right)^2 + \frac{\sigma_{22}^2}{|X_{2t}X_{2c}|} + \left(\frac{\sigma_{12}}{S_{12}}\right)^2\right] + \sigma_{22} \left(\frac{1}{X_{2t}} + \frac{1}{X_{2c}}\right) = 1 \quad (7)$$

$$\sigma_{22} + \sigma_{33} > 0, d_{mt} = 1$$

$$\sigma_{22} + \sigma_{33} < 0, d_{mc} = 1$$

where, $\sigma_{11}, \sigma_{22}, \sigma_{33}, \sigma_{12}$ are components of the stress tensors at an integration point of an element. Next, the damage variables associated with failure modes in fibre tension, fibre compression, matrix tension and matrix compression were denoted as d_{ft}, d_{fc}, d_{mt} and d_{mc} respectively. X_{1t}, X_{2t} and X_{2c} are tensile failure stress in fibre direction, tensile failure stress in direction 2 (transverse to the fibre direction) and compressive failure stress in direction 2, respectively, while S_{11}, S_{12} and S_{13} are shear failures stresses in 1-2, 2-3 and 1-3 planes, respectively [22].

In drilling simulations, the method of element deletion was used to remove the elements from the mesh based on the value of damage variables as calculated from Eq. (1-7) and applied to discrete damage modes in the modelled CFRP composite material. The element was removed when the maximum damage condition was contented at all of the section points at any integration point location of an element [18,22].

Delamination factor

The delamination factor, F_d will be calculated based on Eq. (8). Where d_{max} and d represent is the maximum delaminated diameter and nominal diameter respectively [9].

$$F_d = \frac{d_{max}}{d} \quad (8)$$

Geometry and Meshing

The CFRP composite laminate with overall dimensions of 10 mm × 10 mm × 2 mm was modelled in an individual ply thickness of 0.125 mm with a total of 16 plies as to replicated the experiment performed by Phadnis et al. [18]. The composite laminate was assigned as an explicit 3D deformable part and solid homogeneous. The element sizes at composite laminate are 0.20 mm which was modelled by an 8-node linear brick, one element with 8 nodes (C3D8R), reduced integration and enhanced hourglass control with the total number of elements produced is 89,728.

A backing plate with overall dimensions 12 mm × 12 mm × 0.3 mm with the through the centre hole of diameter 6 mm was modelled as a discrete rigid body with an inertia mass 0.4 kg for support features to the CFRP composite laminate plate during the drilling process. The through-hole was created to reduce and avoid delamination from being occurring during the drilling process. The backing plate was modelled with 4 nodes, 3D bilinear rigid quadrilateral element type (R3D4) and the approximate element size applied was 0.5 mm. A two flutes drill bit with the helix angle and bit point angle of 22.63° and 60.5° with diameter 3 mm was also modelled as a discrete rigid body to reduce the computational efforts required to discretise the complex drill geometry. The drill bit was modelled with 3 nodes, 3D linear triangular element type (R3D3) and approximate element size of 0.5 mm with a total number of an element is 40.

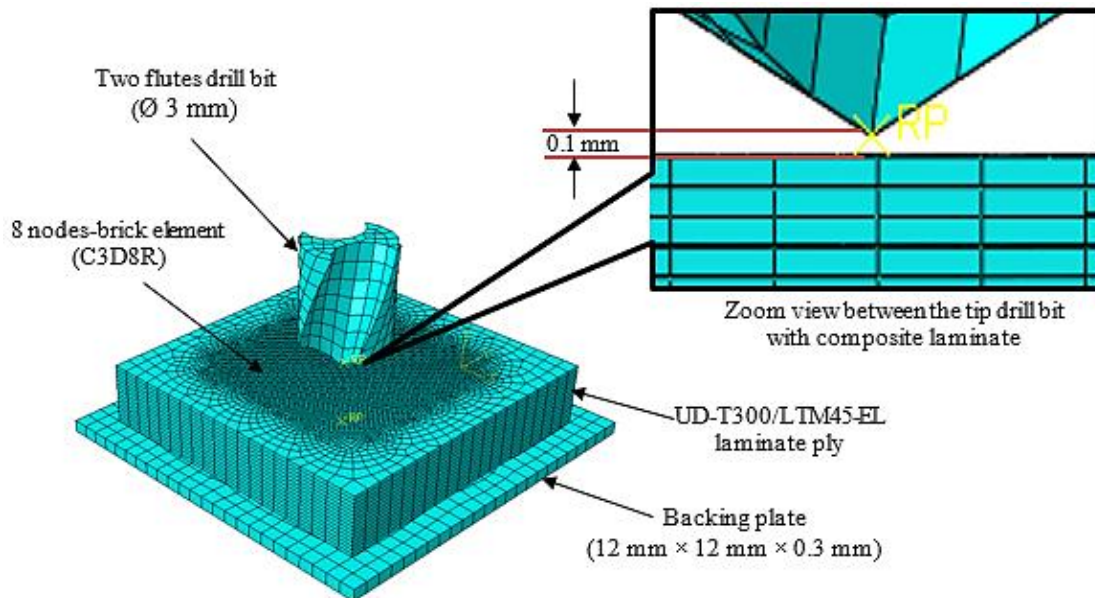


Figure 2. FE model setup of drilling UD-T300/LTM45-EL laminate

In the model, the drill bit was cut extruded and had a total height of 4 mm. A lumped mass and rotary inertia were applied at a reference point located at the chisel edge of the drill bit, to model the kinematics of the drill bit accurately. The drill was modelled with 4 nodes, 3D bilinear rigid quadrilateral element type (R3D4) and the approximate element size applied was 0.5 mm. The laminate composite in this study was stacking by using the different unidirectional fibre ply orientation with a stack sequence of $[0_4/90_8/0_4]$, $[0_4/45_8/0_4]$, $[45_4/90_8/45_4]$, $[45_4/-45_8/45_4]$, $[0/90]_8$, and $[45/-45]_8$. In model assembly, there was a small gap of 0.1 mm between the tip of the drill and composite laminates, this to ensure the drill is fully rotated before contact the laminates as Figure 2 shown.

Boundary Conditions

The drilling feed rate and spindle rotations were applied at a reference point using velocity boundary conditions to account for the dynamic characteristics of the drilling process. While boundary conditions of encastre ($U_1 = U_2 = U_3 = UR_1 = UR_2 = UR_3 = 0$) was applied at the backing plate surface and all four side surfaces of CFRP composite laminate plate to fixed the position. The reference point for a backing plate was selected at the centre surface of the backing plate while the reference point for the drill bit was selected at the chisel edge of the drill bit. A reference point at the drill tip was constrained in X and Y directions while axial velocity corresponding to the imposed feed rate was applied in the Z direction. The reference point on the drill is important to determine the depth of cut of the composite plate [18,22]. The

drill was also made to rotate about Z-axis for angular velocity while rotational degrees of freedom about X and Y directions were constrained.

Contacts and Interactions

There were two types of interaction assigned in the model, which were surface to surface contact and general contact. The general contact interaction was applied in between the surface of ply, and ply with the cohesive property assigned in between the surface contact. The surface to surface was applied to the surface of the drill bit as master surface and CFRP composite plate as the slave surface.

Figure 3 shows the number surface is defined between ply for composite orientation $[0_4/90_8/0_4]$. In between the surface and surface, there was a cohesive surface with the property. Since the cohesive assigned in this model was cohesive surface. Therefore the thickness of the cohesive was negligible and did not give effect to the total thickness of composite which was opposed to the cohesive element. Contact interaction property such as tangential behaviour, cohesive behaviour and damage were applied for modelling a cohesive strength between ply. The value of the friction coefficient under tangential behaviour selection is 0.6. While the value for cohesive behaviour and damage was based on LTM45-EL epoxy data study by Feito et al. [10] as listed in Table 1. The damage initiation and damage evolution are assigned in the interaction property to allow the damage to occur.

Table 1. Properties of cohesive elements for LTM45-EL epoxy

Mechanical Properties	
Stiffness in the normal direction, K_{nn}	200 MPa
Stiffness in shear direction 1, K_{ss}	150 MPa
Stiffness in shear direction 2, K_{tt}	150 MPa
Interface resistance in normal direction, t_n	60 MPa
Interface resistance in shear direction 1, t_s	90 MPa
Interface resistance in shear direction 2, T_t	90 MPa
Rate energy released in the normal direction, G_n^c	0.287 N/mm
Rate energy released in shear direction 1, G_s^c	1.833 N/mm
Rate energy released in shear direction 2, G_t^c	1.833 N/mm

Assumptions and limitations

In developing the Finite Element model, it is critical to follow as close as the experimental set up as well as boundary condition prescription. However, in this computational model, some assumptions were made to simplify the model to reduce the cost of computation and feasible for available computational resources without compromise the acquisition of the outcomes. The precision of the result can be acquired by mesh sensitivity study, whereas the mesh size and shape used are optimal. The balance between computational time and accuracy can be carefully chosen. For material damage behavior in this computational model, the material is assumed as homogenized composite and consider for a fully 3D stress state. During FE analysis, the drill bit and the backing plate were modelled and assumed as discrete rigid bodies. Because there is no specific interest to examine its effect on the drilling process during the simulation, therefore, it was appropriate to model as a rigid body, in order to reduce the overall computational cost and highly time-consuming during drilling simulations [18].

Validation and Sensitivity Analysis

In finite element analysis, firstly a sensitivity study is performed for $[0_4/90_8/0_4]$ ply and validate directly with experimental data from Phadnis et al. [18]. This to prove the simulations parameters and empirical data that apply in this research is converged and lie in the steady zone of sensitivity before it used to predict the others simulation data from different ply orientations sequence. Through convergence and sensitivity study, the results of drilling simulation from being variance may reduce when the factor such as mesh size and step time was determined.

Mesh Size

In meshing analysis, there are six different mesh sizes were examined which are 0.40 mm, 0.35mm, 0.30 mm, 0.25mm, 0.20 mm and 0.15mm. For selecting the proper mesh size, the data of logarithmic strain in each different mesh size model was analyzed. It was observed that the suitable mesh size was lies in the range of 0.20 mm to 0.25 mm. Because at the point of mesh size equal 0.20 mm, the maximum logarithmic strain was converged to a steady-state. Thus, the mesh size

of 0.20 mm x 0.20 mm was selected at the drilling contact area while 0.50 mm x 0.50 mm mesh size was assigned away from the section.

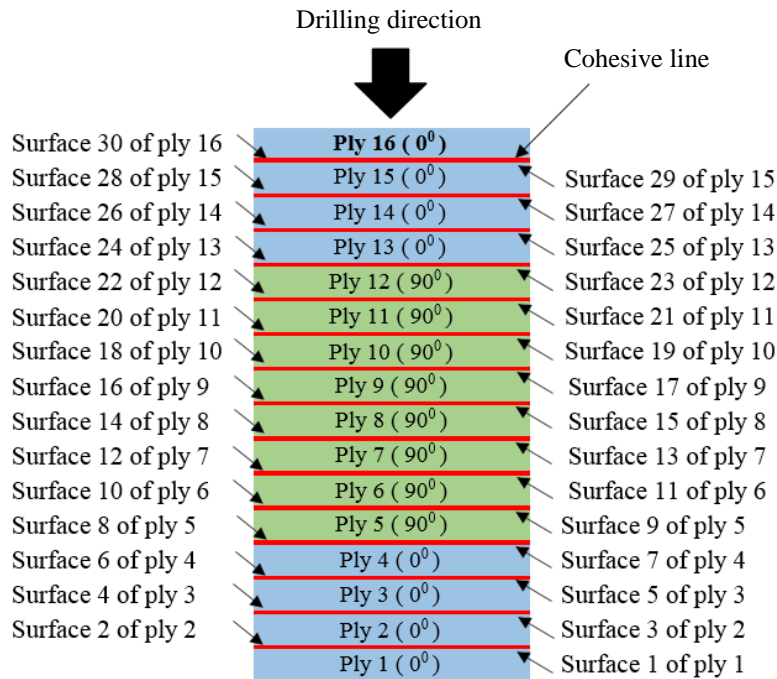


Figure 3. The cohesive property applies between [0₄/90₈/0₄] ply

RESULTS AND DISCUSSION

In order to allow a better comparison of different ply orientation effects in drilling CFRP, a three feed rates of 150 mm/min, 300 mm/min and 500 mm/min with a constant spindle speed of 2500 rpm was chosen from the experimental feed data of ply orientation [0₄/90₈/0₄] which has been indicated by Phadnis et al. [18]. The FE simulations were carried out using these process parameters and later used to validate and predict the thrust force, torque and delamination factor for other feed rates in different ply orientation sequences.

Result Validation

The percentage error between experimental data and simulation data tabulated for [0₄/90₈/0₄] as shown in Table 2 indicate the highest percentage error produced for thrust force and torque was 8.17% at the feed rate of 500 mm/s and 8.47% at the feed rate of 300 mm/s respectively.

Table 2. Summary of percentage error for thrust force and torque

Feed rate (mm/min)	Thrust force (N)			Torque (N.mm)		
	Experiment	FEA	Percentage error (%)	Experiment	FEA	Percentage error (%)
150	114.40	122.51	7.08	67.20	72.50	7.89
300	172.50	182.32	5.69	103.00	111.72	8.47
500	202.10	218.62	8.17	158.00	165.30	4.62

The thrust force comparison between experiment and simulation was plotted in Figure 4. It shows the thrust force gets from the experiment is 8 % lower than the thrust force of simulation. Figure 5 shown the torque comparison between experiment and simulation of [0₄/90₈/0₄]. The torque obtained from the experiment was also 8 % lower than the thrust force of simulation. These comparisons show the FE model provides a good estimation for thrust force and torque. The discrepancy between experiments and the model is less than 10 % [23]. In experiments, several more variable was not be physically modelled in the simulation such as the effect of heat generation and drill wear effect. Another possible reason was, this FEA model uses a constant coefficient of friction throughout the simulation where the average of a set test use for the value. In fact, in the experiment, the coefficient of friction is not consistent. The absence of an accurate friction

coefficient is a limitation in FEA analysis. The inaccuracy of the material can also affect the results of the FE analysis. The element type used to represent the material may also affect results. The default and simplified algorithm scheme available in Abaqus/explicit also gave effect due to mathematical solver simplification [18]. This will be a good topic for further research that can be carried out in another chapter.

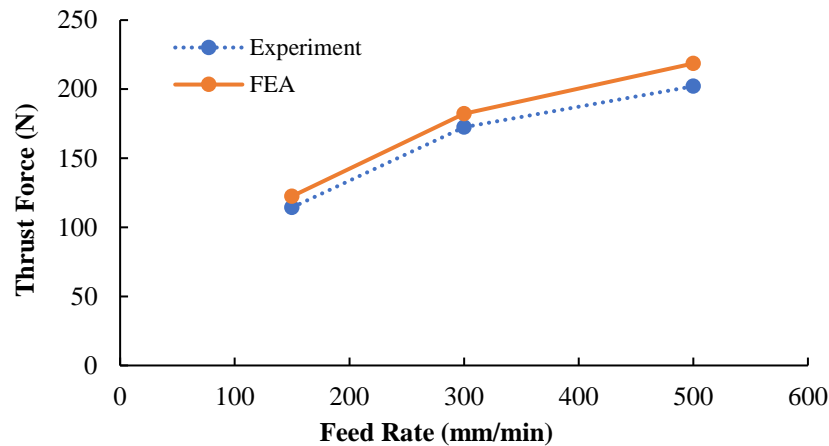


Figure 4. Comparison of thrust force between experiment and simulation for $[0_4/90_8/0_4]$ ply

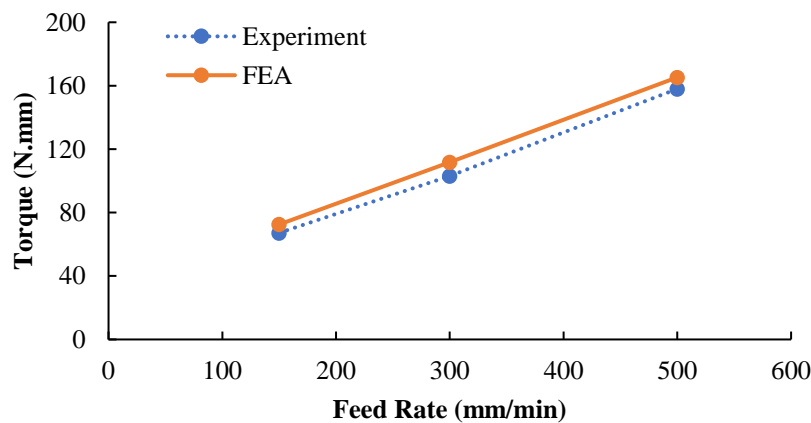


Figure 5. Comparison of torque between experiment and simulation for $[0_4/90_8/0_4]$ ply

Ply Orientation Sequence Analysis

Thrust force and torque

Thrust force is the force of the tool acting toward the axis of the drill to the workpiece. In the model, the reference point was set at the tip of the drill bit to get the result of thrust force against the depth of cut of the composite plate. Figure 6 shows the obtained data from the simulation of thrust force and feed rate in the drilling of UD-T300/LTM45-EL laminate. The graph shows the relationship of thrust force is proportional to feed rate, as the feed rate increase, the thrust force also increase as well. This is due to the larger feed rate, higher will be the cross-sectional area of the undeformed chip, with greater resistance to chip formation and consequently greater axial thrust force [24]. At constant spindle speed of 2500 rpm, the feed rate of 150 mm/min, 300 mm/min and 500 mm/min show that the result of thrust force for ply orientation sequence of $[0_4/45_8/0_4]$ and $[45_4/-45_8/45_4]$ are 401.84 N.mm and 390.53 N.mm respectively as the highest values of thrust force. While the ply orientation of $[0_4/90_8/0_4]$ produce the lowest value which is only 218.62 N.mm compared to other orientation sequences. A uniform amount of fibre material was equally available for drilling using ply orientation $[0_4/90_8/0_4]$, which may result in a smooth cutting operation. However, in the case of ply orientation $[0_4/45_8/0_4]$ and $[45_4/-45_8/45_4]$, interrupted amount of workpiece material was available along the hole periphery, which may have introduced an increased amount of thrust force during the drilling operation [21].

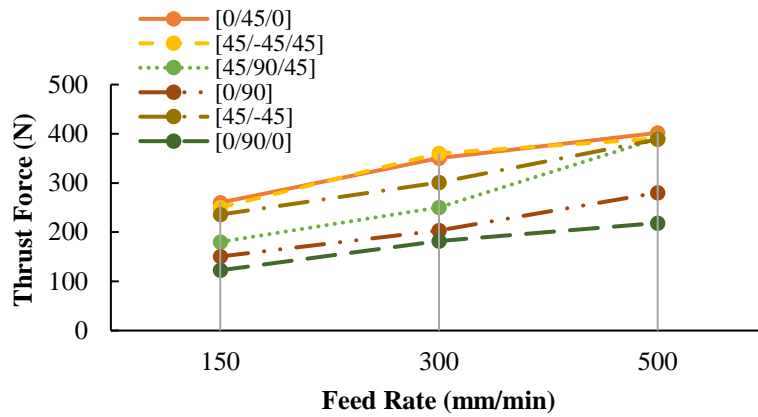


Figure 6. Thrust force in different ply orientations corresponding to feed rates

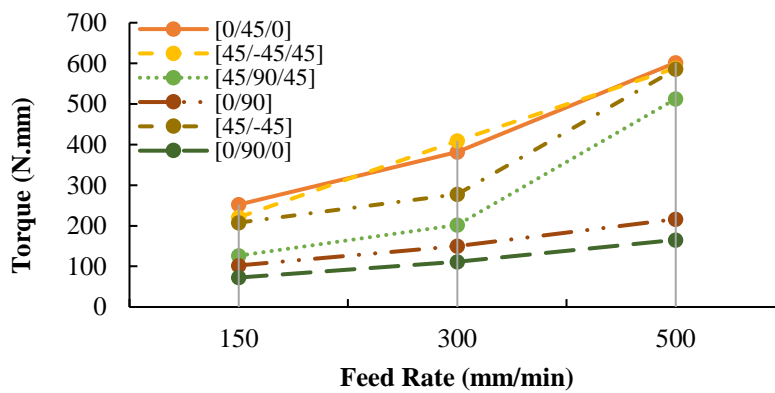


Figure 7. Torque in different ply orientations corresponding to feed rates

Figure 7 shows the drilling torque corresponding to different feed rates. The results indicate that drilling torque increases with an increase in feed rate. The results obtained from FE analysis discovered that torque for the ply orientation sequence of $[0_4/45_8/0_4]$ and $[45_4/-45_8/45_4]$ was the highest with 260.17 N.mm at feed rate 150 mm/min and 401.89 N.mm at 500 mm/min and have almost the same average at a spindle speed of 2500 rpm compared to others orientation sequences. Based on the observation, it shows that all the maximum torque occurred at around 1 mm to 1.5 mm depth of the composite plate which was approximate in the between of ply 8 and plies 12.

Delamination

The delamination factors in this FE analysis were calculated using a simple methodology based on Eq. (8), where the ratio of total number and size of cohesive elements before and after the drilling simulation was calculated. The summary corresponding delamination factors for drill entry and drill exit are listed in Table 3 for all ply orientation sequence. The ply orientation sequence of $[45_4/90_8/45_4]$ produces the highest delamination factor with a significantly increase as feed rate increase compares with the orientation sequence of $[0/90]_8$ that produces the lowest value.

Table 3. Summary of delamination factor in different ply orientations

Ply orientation sequences	Delamination factor (Fd)					
	Feed rate (mm/min)					
	150		300		500	
	At entry	At exit	At entry	At exit	At entry	At exit
[0/90] ₈	0.61	0.68	0.73	0.81	0.77	0.86
[45/-45] ₈	0.78	0.88	0.81	0.96	0.85	0.98
[0 ₄ /90 ₈ /0 ₄]	0.65	0.71	0.69	0.76	0.73	0.87
[0 ₄ /45 ₈ /0 ₄]	0.73	0.85	0.79	0.92	0.86	1.02
[45 ₄ /90 ₈ /45 ₄]	0.81	0.93	0.88	0.97	0.94	1.07
[45 ₄ /-45 ₈ /45 ₄]	0.79	0.87	0.83	0.91	0.88	1.03

It was observed that the higher the feed rate, the higher the stress-induced at the surface of the composite. From the results obtained of ply orientation [0₄/90₈/0₄], noticed that the highest damaged area and stress produced at feed rate 500 mm/min was 309.10 MPa, for feed rate 300 mm/min and 150 mm/min the stress produced is 269.40 MPa and 174.20 MPa respectively as Figure 8 shows the damaged area and stress produced for different feed rate in 2D and 3D view of the composite laminate workpiece in total drilling step time of 1.2 seconds.

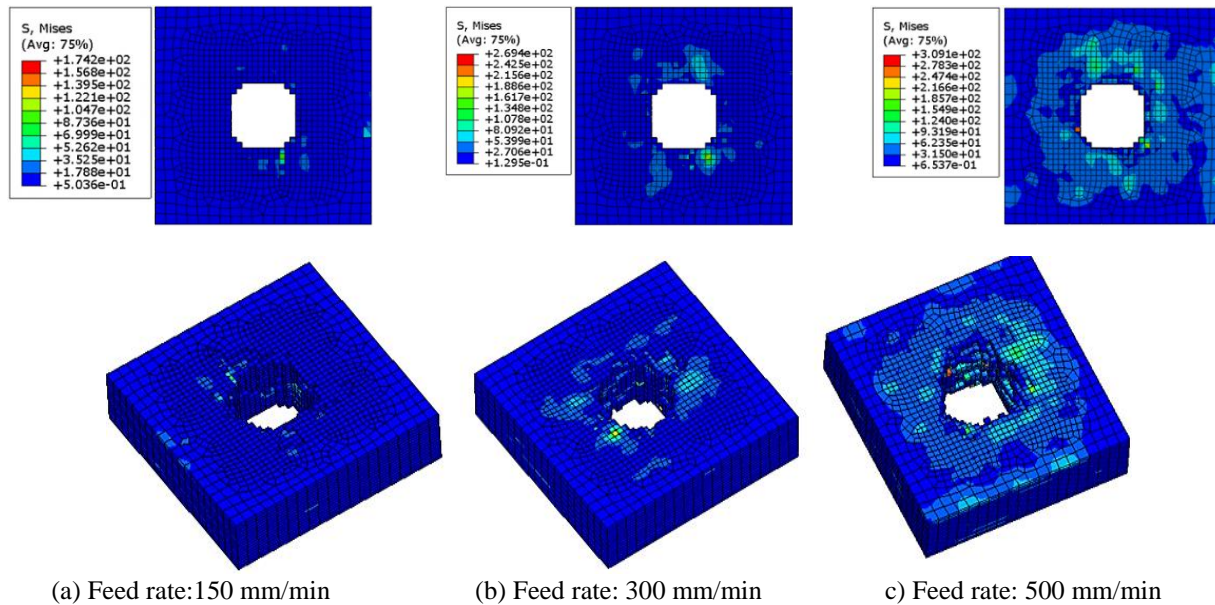


Figure 8. Results of 3D view at the different feed rate for [0₄/90₈/0₄] ply

The delamination factor is higher at the drill exit compare to drill entry as expected. For ply orientation sequence of [0/90]₈ at the feed rate of 150 mm/min, the delamination factor at exist had increased by 8.6 %, while at 300 mm/min and 500 mm/min had increased by about 5.6 % and 4.9 %. The percentage of delamination factor between drill entry and drill exists decreased as the feed rate increase. The highest delamination factor obtains to indicate the bigger the damage induced. Thus, it can be concluded that the suitable feed rate is an important factor in reducing the damage induced in the composite. Practically, the feed rate has to be kept as low as possible to minimize damage extension. Delamination occurs in composite due to the thrust force acting to the composite is greater than the yield strength of the composite [25]. The cohesive element in the composite also plays important roles in delamination.

CONCLUSIONS

In this paper, the effects of discrete machining parameters on thrust force and drilling torque for UD-T300/LTM45-EL composite laminate was investigated numerically and validated by published experiment data for [0₄/90₈/0₄] ply first before continuing simulation for different ply orientations. The primary user-defined material model accounted for an orthotropic material response along with a stress-based damage criterion at the ply-level is implemented using VUMAT subroutine in ABAQUS/EXPLICIT (ABAQUS, Dassault Systèmes®). The method of element–deletion based on the

threshold stress levels in carbon fibre and epoxy matrix materials was implemented in the material model to allow for the hole-making process in drilling. The results proved that the relationship of thrust force is directly proportional to the feed rate with the difference of computational model are 8 % higher than the experiment. Among the ply orientation sequence applied in the simulation, the result shows that $[0_4/45_8/0_4]$ and $[45_4/-45_8/45_4]$ ply having higher thrust force with 401.84 N.mm and 390.53 N.mm at 500 mm/min feed rate as delamination extent, as the frequency of fiber pulls out at the exit region of the drilled hole increases as compared to the restricted fiber ply orientation 0° and 90° . Based on the analysis, thrust force exerted the strongest influence on the damage in the composite. Once the thrust force acting to the composite is greater than the yield strength, the composite will initiate the delamination. The delamination that occurs at the drill exit is always greater than at the drill entry. To minimize the delamination, induce in the composite, the thrust force should be kept as low as possible. It can be concluded; the frequency of fiber pull out at the exit region for 45° fiber orientation types of the drilled hole increases as compared to the restricted fiber ply orientation 0° and 90° .

ACKNOWLEDGEMENT

The authors acknowledge the Faculty of Mechanical Engineering Technology, Universiti Malaysia Perlis, for the lab facilities and financial support.

REFERENCES

- [1] J. Fernández-Pérez, J. L. Cantero, J. Díaz-Álvarez, and M. H. Miguélez, "Influence of cutting parameters on tool wear and hole quality in composite aerospace components drilling," *Compos. Struct.*, vol. 178, pp. 157–161, Oct. 2017, doi: 10.1016/j.compstruct.2017.06.043.
- [2] Z. Mustafa *et al.*, "Optimization of drilling process parameters on delamination factor of Jute reinforced unsaturated polyester composite using Box-Behnken design of experiment," *J. Mech. Eng. Sci.*, vol. 14, no. 1, pp. 6295–6303, 2020, doi: 10.15282/jmes.14.1.2020.08.0493.
- [3] J. Naveen, M. Jawaid, A. Vasanthanathan, and M. Chandrasekar, "Finite element analysis of natural fiber-reinforced polymer composites," in *Modelling of Damage Processes in Biocomposites, Fibre-Reinforced Composites and Hybrid Composites*, Elsevier, 2018, pp. 153–170.
- [4] A. Díaz-Álvarez, M. Rodríguez-Millán, J. Díaz-Álvarez, and M. H. Miguélez, "Experimental analysis of drilling induced damage in aramid composites," *Compos. Struct.*, vol. 202, pp. 1136–1144, Oct. 2018, doi: 10.1016/j.compstruct.2018.05.068.
- [5] H. Li, X. Qin, G. He, M. A. Price, Y. Jin, and D. Sun, "An energy based force prediction method for UD-CFRP orthogonal machining," *Compos. Struct.*, vol. 159, pp. 34–43, Jan. 2017, doi: 10.1016/j.compstruct.2016.09.051.
- [6] M. Altin Karataş and H. Gökkaya, "A review on machinability of carbon fiber reinforced polymer (CFRP) and glass fiber reinforced polymer (GFRP) composite materials," *Defence Technology*, vol. 14, no. 4. China Ordnance Society, pp. 318–326, Aug. 01, 2018, doi: 10.1016/j.dt.2018.02.001.
- [7] L. Durão, J. Tavares, V. de Albuquerque, J. Marques, and O. Andrade, "Drilling Damage in Composite Material," *Materials (Basel)*, vol. 7, no. 5, pp. 3802–3819, May 2014, doi: 10.3390/ma7053802.
- [8] D. Deepak and K. Ashwin Pai, "Study on abrasive water jet drilling for graphite filled glass/epoxy laminates," *J. Mech. Eng. Sci.*, vol. 13, no. 2, pp. 5126–5136, 2019, doi: 10.15282/jmes.13.2.2019.24.0421.
- [9] V. N. Gaitonde, S. R. Karnik, J. C. Rubio, A. E. Correia, A. M. Abrão, and J. P. Davim, "Analysis of parametric influence on delamination in high-speed drilling of carbon fiber reinforced plastic composites," *J. Mater. Process. Technol.*, vol. 203, no. 1–3, pp. 431–438, Jul. 2008, doi: 10.1016/j.jmatprotec.2007.10.050.
- [10] N. Feito, J. López-Puente, C. Santiuste, and M. H. Miguélez, "Numerical prediction of delamination in CFRP drilling," *Compos. Struct.*, vol. 108, no. 1, pp. 677–683, Feb. 2014, doi: 10.1016/j.compstruct.2013.10.014.
- [11] R. Fu *et al.*, "Drill-exit temperature characteristics in drilling of UD and MD CFRP composites based on infrared thermography," *Int. J. Mach. Tools Manuf.*, vol. 135, pp. 24–37, Dec. 2018, doi: 10.1016/j.ijmachtools.2018.08.002.
- [12] N. Feito, J. Díaz-Álvarez, J. López-Puente, and M. H. Miguélez, "Experimental and numerical analysis of step drill bit performance when drilling woven CFRPs," *Compos. Struct.*, vol. 184, pp. 1147–1155, Jan. 2018, doi: 10.1016/j.compstruct.2017.10.061.
- [13] S. M. Bukhari, J. Kandasamy, and M. Manzoor Hussain, "Investigations on drilling process parameters of Hybrid Composites with different stacking sequence," in *Materials Today: Proceedings*, Jan. 2017, vol. 4, no. 2, pp. 2184–2193, doi: 10.1016/j.matpr.2017.02.065.
- [14] D. Wang *et al.*, "Study on damage evaluation and machinability of UD-CFRP for the orthogonal cutting operation using scanning acoustic microscopy and the finite element method," *Materials (Basel)*, vol. 10, no. 2, 2017, doi: 10.3390/ma10020204.
- [15] C. A. Van Luttervelt *et al.*, "Present situation and future trends in modelling of machining operations progress report of the CIRP working group 'modelling of machining operations,'" *CIRP Ann. - Manuf. Technol.*, vol. 47, no. 2, pp. 587–626, Jan. 1998, doi: 10.1016/S0007-8506(07)63244-2.
- [16] M. Mahdi and L. Zhang, "A finite element model for the orthogonal cutting of fiber-reinforced composite materials," in *Journal of Materials Processing Technology*, Jun. 2001, vol. 113, no. 1–3, pp. 373–377, doi: 10.1016/S0924-0136(01)00675-6.

- [17] N. Shetty, S. M. Shahabaz, S. S. Sharma, and S. Divakara Shetty, "A review on finite element method for machining of composite materials," *Composite Structures*, vol. 176. Elsevier Ltd, pp. 790–802, Sep. 15, 2017, doi: 10.1016/j.compstruct.2017.06.012.
- [18] V. A. Phadnis, F. Makhdam, A. Roy, and V. V. Silberschmidt, "Drilling in carbon/epoxy composites: Experimental investigations and finite element implementation," *Compos. Part A Appl. Sci. Manuf.*, vol. 47, no. 1, pp. 41–51, Apr. 2013, doi: 10.1016/j.compositesa.2012.11.020.
- [19] Z. Hashin, "Failure criteria for unidirectional fiber composites," *J. Appl. Mech. Trans. ASME*, vol. 47, no. 2, pp. 329–334, Jun. 1980, doi: 10.1115/1.3153664.
- [20] A. Gherissi, "Failure study of the woven composite material: 2.5 D carbon fabric/ resin epoxy," *J. Mech. Eng. Sci.*, vol. 13, no. 3, pp. 5390–5406, 2019, doi: 10.15282/jmes.13.3.2019.12.0438.
- [21] A. Puck and H. Schürmann, "Failure analysis of FRP laminates by means of physically based phenomenological models," *Compos. Sci. Technol.*, vol. 62, no. 12-13 SPECIAL ISSUE, pp. 1633–1662, Sep. 2002, doi: 10.1016/S0266-3538(01)00208-1.
- [22] Y. L. He, G. P. Zhang, and J. P. Xue, "Finite element analysis on drilling of unidirectional carbon fiber reinforced plastic(CFRP)," in *Applied Mechanics and Materials*, 2014, vol. 455, pp. 228–231, doi: 10.4028/www.scientific.net/AMM.455.228.
- [23] O. Isbilir and E. Ghassemieh, "Finite element analysis of drilling of titanium alloy," in *Procedia Engineering*, Jan. 2011, vol. 10, pp. 1877–1882, doi: 10.1016/j.proeng.2011.04.312.
- [24] C. C. Tsao and Y. C. Chiu, "Evaluation of drilling parameters on thrust force in drilling carbon fiber reinforced plastic (CFRP) composite laminates using compound core-special drills," *Int. J. Mach. Tools Manuf.*, vol. 51, no. 9, pp. 740–744, Sep. 2011, doi: 10.1016/j.ijmachtools.2011.05.004.
- [25] K. Phapale, S. Patil, R. Singh, and R. K. P. Singh, "Comparative study of drilling induced delamination in CFRP with different ply orientation," in *Key Engineering Materials*, 2016, vol. 705, pp. 227–232, doi: 10.4028/www.scientific.net/KEM.705.227.